

Cite this: *RSC Advances*, 2012, 2, 7759–7771

www.rsc.org/advances

PAPER

Improving therapeutic effect in ovarian peritoneal carcinomatosis with honokiol nanoparticles in a thermosensitive hydrogel composite†

Yao Xie,^{ab} Qida Long,^{‡ac} QinJie Wu,^a Shuai Shi,^a Mei Dai,^a Yingwei Liu,^b Lei Liu,^a Changyang Gong,^{*a} Zhiyong Qian,^a Yuquan Wei^a and Xia Zhao^{*a}

Received 3rd April 2012, Accepted 25th June 2012

DOI: 10.1039/c2ra20612a

Ovarian cancer is one of the most common carcinomas and causes lots of deaths in the world. Honokiol (HK), a natural product, was proved to be a potent anti-tumor agent, however the hydrophobicity of HK limited its application. In this work, we investigated the anti-tumor efficacy of honokiol nanoparticles (HK-NPs) and honokiol nanoparticles-loaded thermosensitive hydrogel (HK-NPs/hydrogel) on ovarian cancer *in vitro* and *in vivo*. HK-NPs with small particle size and high drug loading were prepared, and HK-NPs/hydrogel with a sol–gel transition temperature at about body temperature was also obtained. In addition, HK-NPs and HK-NPs/hydrogel showed a sustained release behavior of HK *in vitro*. HK-NPs could effectively inhibit proliferation of SKOV3 tumor cells in a dose- and time-dependent manner and induce apoptosis of tumor cells *in vitro*. Furthermore, compared with controlled groups, HK-NPs and HK-NPs/hydrogel dramatically inhibited growth of tumors and prolonged the survival of mice bearing ovarian peritoneal carcinomatosis (OPC), and the effects of HK-NPs/hydrogel were more obvious than HK-NPs ($P < 0.05$). Intraperitoneal chemotherapy with HK-NPs/hydrogel significantly inhibited proliferation activity and angiogenesis of tumors and increased apoptosis and necrosis in tumor tissues. Therefore, our results suggested that HK-NPs/hydrogel may have great potential in clinical applications in the treatment of OPC.

1. Introduction

Ovarian cancer is the most lethal and the second most common gynecologic malignancy in the United States, which accounts for nearly half of all gynecological cancer deaths.¹ The majority of patients with ovarian cancer presenting advanced stages of the disease are treated with a combination of surgery and intravenous systemic paclitaxel and platinum-based chemotherapy.² The high incidence of chemotherapy resistance limits the effect of chemotherapy. Therefore, new treatment strategies are needed to increase the effectiveness of conventional cytotoxic chemotherapy and to overcome chemo-resistance with minimal toxicity.³

Although multicenter, randomized, phase III clinical trials have shown that intraperitoneal (IP) chemotherapy is superior to standard intravenous chemotherapy for patients with small volume, residual, advanced epithelial ovarian cancer,^{4–6} and that IP chemotherapy for advanced ovarian cancer improves both the overall and disease-free survival,⁷ there are several barriers to implementation of this treatment into clinical practice, including toxicity concerns and a lack of technical expertise with the peritoneal infusion device.^{8–10}

The root and stem bark of *magnolia officinalis* has traditionally been used to treat thrombotic stroke, gastrointestinal complaints, anxiety and nervous disturbance by Chinese people. Honokiol (HK) is one of the major phenolic constituents of magnolia bark. In recent years, the pharmacological effects of HK have been demonstrated, such as acting as an anti-oxidant, an antithrombotic and antibacterial agent and causing inhibition of xanthine oxidase as well as showing anxiolytic effects. The remarkable anti-tumor effects of HK were also revealed. Previous reports proved its activities on human colon cancer,¹¹ neuroblastoma,¹² osteosarcoma,¹³ breast cancer,¹⁴ melanoma cells,¹⁵ pancreatic cancer cells,¹⁶ hepatocellular carcinoma cells,¹⁷ leukemia cells,¹⁸ lung cancer¹⁹ and ovarian cancer,^{20,21} in which the induction of apoptosis may be involved.

However, due to the poor water-solubility, HK was dissolved in dimethyl sulfoxide (DMSO) for research in most studies. Its

^aState Key Laboratory of Biotherapy, West China Hospital, and Department of Gynecology and Obstetrics, Second West China Hospital, Sichuan University, Chengdu, 610041, China.

E-mail: chygong14@yahoo.com.cn; xia-zhao@126.com;

Fax: +86 28 85164060; Tel: +86 28 85164063

^bDepartment of Obstetrics and Gynecology, the Southwest Hospital of the Third Military Medical University, Chongqing, 400038, China

^cDepartment of Obstetrics and Gynecology, Guangzhou Women and Childrens' Medical center, Guangzhou, 510623, China

† Electronic supplementary information (ESI) available. See DOI: 10.1039/c2ra20612a

‡ Q Long and Y Xie contributed equally to this paper, and Q Long is the co-first author of this paper.

application in clinical practice was greatly restrained. In order to develop the aqueous formulation of HK, HK-NPs were prepared by emulsion solvent evaporation in our laboratory.

As a controlled drug delivery system (DDS) for IP chemotherapy, biodegradable poly(ethylene glycol)-poly(ϵ -caprolactone)-poly(ethylene glycol) (PEG-PCL-PEG, PECE) thermosensitive hydrogel was synthesized in previous work.^{22–24} PECE hydrogel is a free-flowing sol at room temperature and becomes a non-flowing gel at body temperature, serving as a drug depot *in situ*. Instead of a peritoneal infusion device, thermosensitive PECE hydrogel is an injectable DDS.

The present study aimed to determine whether (1) HK-NPs could inhibit the growth of ovarian cancer SKOV3 cells *in vitro* and *in vivo* and (2) as a novel controlled dosage form, the polymeric matrix HK-NPs/hydrogel for IP chemotherapy prolonged the survival of mice bearing ovarian peritoneal carcinomatosis (OPC) and showed more obvious anti-tumor effects.

2. Materials and methods

2.1 Materials, cell lines, and animals

Pluronic® F127 (Sigma, USA), poly(ethylene glycol) methyl ether (MPEG, Aldrich, USA), ϵ -caprolactone (ϵ -CL, Aldrich, USA), hexamethylene diisocyanate (HMDI, Aldrich, USA), stannous octoate (Sn(Oct)₂, Sigma, USA), propidium iodide (PI, Sigma, USA), RNase A (Sigma, USA), DMSO (Sigma, USA), 3-(4,5-dimethyl-2-thiazolyl)-2, 5-diphenyl-2H-tetrazolium bromide (methyl thiazolyl tetrazolium, MTT, Sigma, USA), Roswell Park Memorial Institute 1640 medium (RPMI 1640, Gibco, USA), L-glutamine (Gibco, USA), fetal bovine serum (FBS, Gibco, USA), amikacin (TaKaRa, USA), trypsin (Invitrogen, USA) and *in situ* cell death detection kits (Roche, Switzerland) were used as received. Primary antibodies were mouse anti-CD34 Class II (Gene Tech) and mouse anti-proliferating cell nuclear antigen (PCNA) clone PC 10 (Invitrogen). Secondary antibodies for colorimetric immunohistochemical analysis were biotinylated goat anti-rat immunoglobulin and goat anti-mouse IgG (BD Biosciences Pharmingen). The substrate buffer was 3-amino-9-ethylcarbazole (AEC) substrate kit. All other reagents used were all analytical reagents.

The human ovarian cancer cell line, SKOV3, derived from a papillary serous cystadenocarcinoma of human ovary,²⁵ was purchased from American Type Culture Collection (ATCC, Rockville, Maryland) and grew in RPMI 1640 with 10% FBS, 2 Mm L-glutamine and 0.1 mg ml⁻¹ Amikacin, at 37 °C in a humidified atmosphere of 5% CO₂.

Female athymic nude mice (BALB/c), 6–8 weeks old, were purchased from the Vital River Lab Animal Technology Co., Ltd. (Beijing, China). Mice were housed and maintained in a specific sterile environment in the Laboratory Animal Center, National Key Laboratory of Biotherapy and Cancer Center, Sichuan University, and cared for in accordance with current guidelines. All the studies were approved and supervised by the Sichuan University Institutional Animal Care and Use Committee.

2.2 Preparation and characterization of honokiol nanoparticles (HK-NPs)

HK-NPs were prepared by the emulsion solvent evaporation method described in our previous work.²⁶ In brief, HK crystals

(Sikehua Biotechnology, Chengdu, China) were dissolved in ethyl acetate, and the solution was induced into a Pluronic® F127 aqueous solution. Excessive stirring allowed this mixture to form an oil-in-water emulsion. When ethyl acetate was evaporated in a rotatory evaporator, HK-NPs were obtained.

Drug loading (DL) and encapsulation efficiency (EE) of HK-NPs were determined as follows. Briefly, 10 mg of lyophilized HK-NPs were dissolved in 0.1 mL of acetonitrile. The amount of HK in the solution was determined by high performance liquid chromatography (HPLC). The DL and EE of HK-NPs were calculated according to eqn (1) and (2):

$$DL = \frac{\text{Drug}}{\text{Polymer} + \text{Drug}} \times 100\% \quad (1)$$

$$EE = \frac{\text{Experimental drug loading}}{\text{Theoretical drug loading}} \times 100\% \quad (2)$$

The particle size of prepared HK-NPs was determined by a Malvern Nano-ZS 90 laser particle size analyzer after equilibration for 10 min. All results were the mean of three test runs, and all data were expressed as the mean \pm standard deviation (SD).

The morphological characteristics of the HK-NPs were examined by a transmission electron microscope (TEM, H-6009IV, Hitachi, Japan). The HK-NPs were diluted with distilled water and placed on a copper grid covered with nitrocellulose. The sample was negatively stained with phosphotungstic acid and dried at room temperature.

2.3 Preparation and characterization of hydrogel and HK-NPs loaded hydrogel (HK-NPs/hydrogel)

Biodegradable PECE triblock copolymer was synthesized in our laboratory by ring-opening polymerization as described previously.²⁷ The obtained PECE copolymers were characterized by Fourier transform infrared spectroscopy (FTIR, NICOLET 200SXV, Nicolet, USA), ¹H nuclear magnetic resonance spectroscopy (¹H-NMR, Varian 400 spectrometer, Varian, USA) and gel permeation chromatography (GPC, Agilent 110 HPLC, USA).

To prepare HK-NPs/hydrogel, PECE copolymer was dissolved well in water at a certain temperature and cooled to 4 °C to form injectable and biodegradable thermosensitive hydrogel. Then, the obtained HK-NPs were mixed with PECE hydrogel to form the HK-NPs/hydrogel composite, and the concentration of PECE copolymer was kept at 30% wt.

The sol–gel–sol phase transition behaviors of thermosensitive PECE hydrogel and HK-NPs/hydrogel were studied using a test tube-inverting method with a 4 ml tightly screw-capped vial with an inner diameter of 10 mm. The sol–gel–sol transition was visually observed by inverting the vials, and conditions of gel and sol were defined as “no flow” and “flow” in one minute respectively. The volume of the hydrogel samples containing different contents of HK-NPs was kept at 1 mL in total regardless of the micelles content. The hydrogel samples were slowly heated at a heating rate of 1 °C min⁻¹, from 4 °C to the temperature when precipitation occurred.

In vitro release behaviors of HK from HK-NPs or HK-NPs/hydrogel were investigated by a modified dialysis method.

HK-NPs or HK-NPs/hydrogel (30 wt%) were placed in a dialysis tube (molecular mass cutoff is 3.5 kDa), and HK solution in DMSO (1 mg mL⁻¹) was used as the control. The dialysis tubes were incubated in 10 mL of PBS (pre-warmed to 37 °C, pH = 7.4) containing Tween 80 (0.5% wt) at 37 °C with gentle shaking (100 rpm). The media were displaced by pre-warmed fresh PBS at a predetermined time. After centrifugation, the supernatant of the removed release media was collected and stored at -20 °C until analysis. The released drug was quantified using HPLC. All results were the mean of three test runs, and all data were expressed as the mean ± SD.

The concentration of HK was determined by HPLC (Waters Alliance 2695) and samples were diluted before measurement. The solvent delivery system was equipped with a column heater and a plus autosampler. Detection was done with a Waters 2996 detector. Chromatographic separations were performed on a reversed phase C₁₈ column (4.6 × 150 mm-5 μm, Sunfire Analysis column). And the column temperature was kept at 28 °C. Acetonitrile/water (60/40, v/v) was used as the eluent at a flow rate of 1 mL min⁻¹.

2.4 *In vitro* cell proliferation assay

Colorimetric assays were performed to evaluate the activity of HK-NPs and free HK using the standard MTT assay.^{28,29} *In vitro* cytotoxicity of Pluronic® F127 and PECE copolymer was also tested. SKOV3 cells incubated in 96-well plates were treated with the indicated concentration of HK-NPs, free HK, Pluronic® F127 and PECE copolymer for 24 h and 48 h. Cells not treated with reagents were used as negative controls. Optical densities (OD) at a wavelength of 570 nm were quantified on an enzyme-labeled instrument (Microplate Reader 3550-UV, BIO-RAD). The mean percentage of cell survival relative to that of untreated cells was estimated from data of six individual experiments, and all data were expressed as the mean ± SD.

2.5 DNA fragmentation assay

DNA cleavage and fragmentation was analyzed by agarose gel electrophoresis as previously described.³⁰ SKOV3 cells were treated with either 12.5 μg mL⁻¹ or 20 μg mL⁻¹ of HK-NPs for 36 h. Cells were harvested, washed with PBS, lysed with 200 μL lysis buffer (50 mM Tris-HCl pH = 8, 20 mM EDTA, 0.25% Nonidet P-40), and then RNase A was added to a final concentration of 200 μg mL⁻¹ and further incubated in a water bath at 37 °C for 90 min. After addition of proteinase K to a final concentration of 300 μg mL⁻¹ and incubation in a water bath for another 90 min, 15 μL DNA samples were diluted with 4 μL loading buffer and an apoptotic DNA ladder (Invitrogen) were electrophoresed (50 V for 2 h) on 1.5% agarose gel. The gel was then stained with 0.1 μg mL⁻¹ ethidium bromide and viewed using a gel imaging system (Gel Doc 1000, BIO-RAD & Video Copy Processor, Mitsubishi).

2.6 Propidium iodide (PI) DNA staining

The morphological detection of chromosomal DNA stained with PI was used to confirm the apoptotic effect of HK-NPs. SKOV3 cells incubated in 6-well plates were treated with 12.5 mg mL⁻¹

of HK-NPs, Pluronic® F127 and PECE copolymer in 2 mL RPMI-1640 for 48 h. 2 mL RPMI-1640 without treatment reagents were added as controls. After removal of the compounds, cells were rinsed with PBS, fixed with pre-chilled 70% ethanol for 30 min at room temperature, rinsed with PBS twice and stained with 0.5 mL PI (5 μg/mL in PBS) for 10 min. Chromatin fluorescence was observed under fluorescence microscopy (TE2000-U, Nikon) at excitation 535 nm/emission 615 nm wavelengths. Apoptotic cells demonstrated cytoplasmic and nuclear shrinkage and chromatin condensation.

2.7 Flow cytometry assay

To further confirm the apoptotic effect of HK-NPs, a flow cytometry assay was performed. SKOV3 cells cultured in 6-well plates were treated with 12.5 mg mL⁻¹ of HK-NPs, Pluronic® F127, and PECE copolymer in 2 mL RPMI-1640 for 48 h. 2 mL RPMI-1640 without treatment reagents were added as the control. When cells were harvested, they were washed with PBS, fixed with pre-chilled 70% ethanol for 30 min, pretreated with 20 μL RNase I (250 μg mL⁻¹) and stained with 200 μL PI (50 μg mL⁻¹) for 30 min. Cell apoptosis was analyzed with a flow cytometer (EPICS Elite ESP, Beckman Coulter, USA).^{30,31}

2.8 *In vivo* mouse model and treatment plan

Before the treatment of HK-NPs, the maximum tolerated dose (MTD) of HK-NPs based on intraperitoneal injection was determined using athymic nude mice. We found that the MTD of HK-NPs was 200 mg Kg⁻¹, and when the dose of HK-NPs was higher than 30 mg Kg⁻¹, mice showed signs of uncomfartableness. Therefore, 10 mg Kg⁻¹ was chosen in the *in vivo* anti-tumor experiments.

To establish the *in vivo* OPC mouse model,³² SKOV3 cells were harvested during the log growth phase and injected subcutaneously in the backs of five nude mice at a concentration of 5 × 10⁶ cells/0.1 mL of serum-free RPMI-1640. Six weeks later, when the diameters of tumors on the backs of the mice were approximately 1–1.5 cm, the five mice were sacrificed. Tumors were harvested by excising the necrotic tissue and connective tissue, which was then minced into <1 mm³ small particles that could be drawn smoothly using a 14-gauge needle. 12 mL serum-free RPMI-1640 was added. Forty mice were injected intraperitoneally with 0.3 mL of the tumor suspension, which was vigorously vibrated before each injection.

Seven days after the intraperitoneal tumor suspension injection, mice were randomly assigned to six treatment groups (*n* = 10 per group, 5 for tumor growth inhibition study and 5 for survival periods study): 200 μL normal saline (NS) was injected intraperitoneally once weekly, 200 μL blank nanoparticles in PECE hydrogel (NPs/hydrogel) was injected intraperitoneally once weekly, 200 μL free HK (containing HK 10 mg kg⁻¹) was injected intraperitoneally once weekly, 200 μL HK-NPs (containing HK 10 mg kg⁻¹) was injected intravenously (iv) once weekly, 200 μL HK-NPs (containing HK 10 mg kg⁻¹) was injected intraperitoneally once weekly, and 200 μL HK-NPs/hydrogel (containing HK 10 mg kg⁻¹) was injected intraperitoneally once weekly. For the tumor growth inhibition study, mice (5 mice per group) were monitored for general health status every day, the mice were weighed every 3 days, and they were

sacrificed on day 31. Tumor distribution and tumor weight were recorded. Tissue specimens were fixed in formalin for paraffin embedding. Immunohistochemical analysis was performed. To further study the therapeutic effect against ovarian cancer, survival times of the mice were observed (5 mice per group).

Mice treated with HK-NPs and HK-NPs/hydrogel were investigated for potential toxicity. The fur, appetite, status and behavior were observed. Tissues of the heart, lung, liver, spleen, kidney, and intestine were fixed in 10% buffered formalin solution and embedded in paraffin. Sections were stained with hematoxylin and eosin (H&E) and examined under light microscopy.

2.9 Apoptotic tumor cells detection

Terminal deoxynucleotidyl transferase-mediated dUTP nick-end labeling (TUNEL) staining was performed with an *in situ* cell death detection kit according to the manufacturer's directions (Roche). Images of the representative tissue sections were taken by using an OLYMPUS BX600 microscope and a SPOT FIEIX camera. The number of TUNEL-positive cells was counted in 10 random 0.011 mm² fields at ×400 magnification.

2.10 Immunohistochemical determination of CD34 and PCNA

Paraffin embedded tumor tissue was sliced into sections for quantification of microvessel density (MVD) and PCNA using the labeled streptavidin-biotin method.³³ The primary antibody was rat anti-mouse CD34 (Gene Tech) and the secondary antibody was biotinylated goat anti-rat immunoglobulin (BD Biosciences Pharmingen). Images of tumor tissue and microvessels were taken by an OLYMPUS BX600 microscope and SPOT FIEIX camera. A single microvessel was defined as a discrete cluster or single cell that stained positive for CD34, and the presence of a lumen was required for scoring as a microvessel. To quantify MVD, 10 random 0.159 mm² fields at ×100 magnification were examined for each tumor (one slide per mouse, five slides per group) and counted by two independent investigators in a blinded fashion.

The slides for immunohistochemistry of PCNA were treated in the same way but the primary antibody was mouse anti-human PCNA (Invitrogen) and the secondary antibody was biotinylated goat anti-mouse IgG (BD Biosciences Pharmingen). To quantify PCNA expression, the PCNA labelling index (PCNA LI) was calculated as the number of PCNA-positive cells/total number of cells counted under ×400 magnification in five randomly selected areas in each tumor sample.

2.11 Statistical analyses

The statistical analysis software SPSS13.0 for Windows (SPSS Inc., Chicago, IL) was used. The results are recorded as mean ± SD. ANOVA were employed for multiple group comparisons. The nude mice survival time were curved by the Kaplan-Meier method and analysed by a log-rank test. P < 0.05 was considered statistically significant.

3 Results

3.1 Preparation and characterization of HK-NPs

HK was encapsulated into F127 nanoparticles using an emulsion solvent evaporation method. According to Fig. 1A and B,

average particle size, polydispersity (PDI), and zeta potential of obtained HK-NPs were 33.36 ± 2.42 nm, 0.045 ± 0.018 , and -0.270 ± 0.127 mV, respectively. Fig. 1C shows the TEM image of HK-NPs, and the TEM image revealed that HK-NPs were monodisperse with spherical shapes. The diameter of HK-NPs observed by TEM was in good agreement with the results of the particle size. The appearance of prepared HK-NPs is presented in Fig. 1D, and a stable and homogeneous solution of HK-NPs could be observed. Moreover, the HK-NPs can be lyophilized into a powder form without any adjuvant, and the re-dissolved HK-NPs are stable and homogeneous. The drug loading and encapsulation efficiency of the prepared HK-NPs are $14.92 \pm 0.06\%$ and $99.13 \pm 0.31\%$, respectively.

3.2 Preparation and characterization of HK-NPs/hydrogel

A biodegradable PECE triblock copolymer was successfully synthesized,^{34,35} and the molecular weight of PECE copolymer, calculated from ¹H-NMR spectra, was 3408 (PEG/PCL = 960/2448).

PECE hydrogel based on a central PCL block and end PEG blocks exhibited a temperature-dependent sol–gel transition (lower transition) and gel–sol transition (upper transition). The hydrogel is a free-flowing sol at low temperature, but converts into non-flowing gel at body temperatures about 37 °C. After HK-NPs were well incorporated into hydrogel at low temperature, the injectable homogeneous HK-NPs/hydrogel was obtained (Fig. 2A-a). With increase of temperature, HK-NPs/hydrogel became an opaque gel at 37 °C (Fig. 2A-b).

The sol–gel–sol phase transition diagram of HK-NPs/hydrogel is presented in Fig. 2B. The hydrogel system had lower critical gelation temperature (LCGT, the temperature at which the lower sol–gel phase transition occurs), and upper critical gelation temperature (UCGT, the temperature at which the upper gel–sol phase transition occurs). When different amounts of HK-NPs were incorporated into the hydrogel, the effect of the amount of HK-NPs on the sol–gel transition temperature was investigated and the result is shown in Fig. 2B. With an increase in amount of HK-NPs, the LCGT decreased slightly and the UCGT increased gradually, which meant the gelation window became wider. The sol–gel phase transition behavior of the PECE copolymer-based thermosensitive hydrogel is associated with micellar aggregation. The incorporated polymeric nanoparticles may interact with the micellar structure of the hydrogel, thus affecting the phase transition temperature of the hydrogel system.

In vitro drug release behavior of HK from HK-NPs and HK-NPs/hydrogel were presented in Fig. 2C and free HK (dissolved in DMSO) was used as the control. Compared with the rapid release of free HK, a much slower and sustained release of HK-NPs and HK-NPs/hydrogel were observed. Moreover, the cumulative release rate of HK-NPs/hydrogel was much slower than that of HK-NPs. These sustained drug release behaviors indicated their potential applicability as a drug delivery system to minimize the exposure of healthy tissues while increasing the accumulation of therapeutic drug in the tumor site.

3.3 HK-NPs inhibit SKOV3 cell proliferation and induce apoptosis *in vitro*

To identify the therapeutic potential of HK-NPs, SKOV3 cells were cultured with HK-NPs for 24 h and 48 h. F127, the

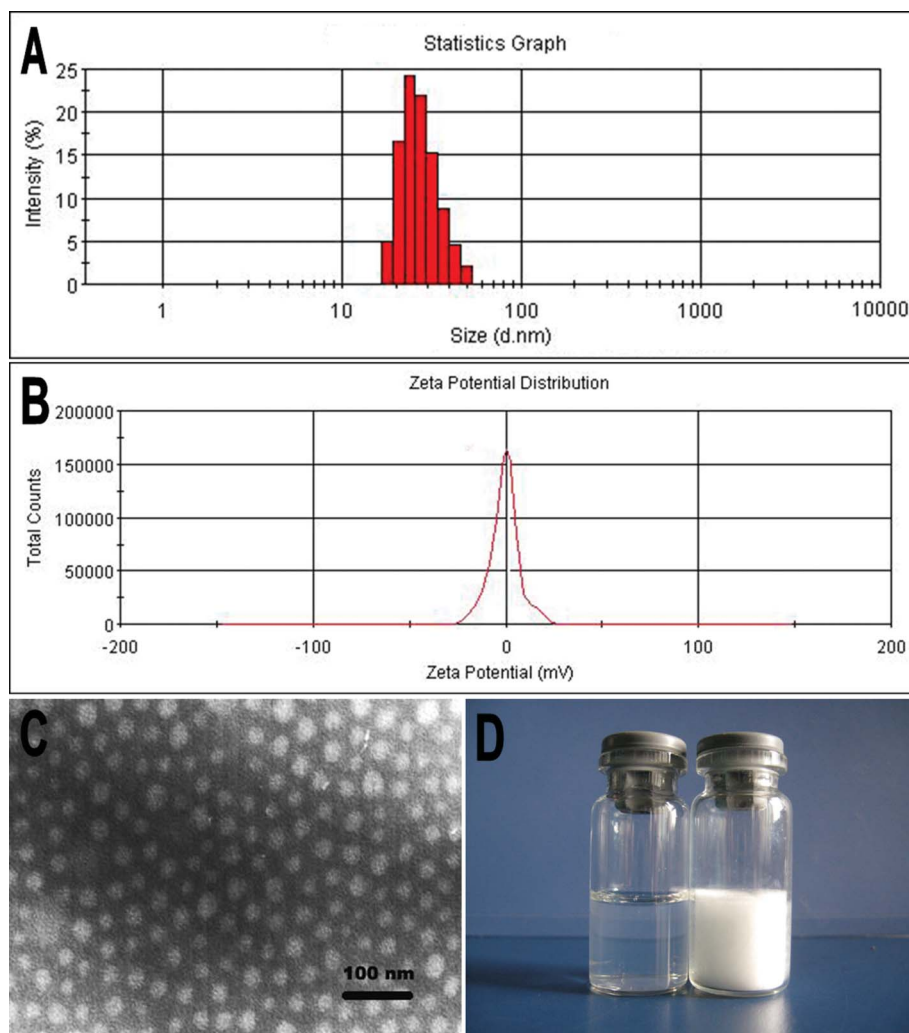


Fig. 1 Preparation and characterization of HK-NPs. A: Particles size distribution of HK-NPs. B: Zeta potential of HK-NPs. C: TEM image of HK-NPs. D: Morphology of HK-NPs (left) and freeze-dried powder of HK-NPs (right).

composition of HK-NPs and PECE hydrogel were also investigated (Fig. 3C and D). The anti-proliferative effect of HK-NPs shows a dose-dependent response and a time-dependent response. The effect of HK-NPs was better than that of free HK dissolved in DMSO as shown in Fig. 3A and B. F127 and PECE copolymers showed a very low cytotoxicity on SKOV3 cells.

A DNA fragmentation assay, *in situ* PI DNA staining, and a flow cytometry assay were used to obtain indications that HK-NPs induced apoptosis in SKOV3 cells. As a hallmark of cells undergoing apoptosis in HK-NPs-treated SKOV3 cells, there was a ladder-like pattern of DNA fragments observed on agarose gels, which consisted of internucleosomal DNA fragments of approximately 180–200 base pairs. SKOV3 cells treated with $12.5 \mu\text{g mL}^{-1}$ HK-NPs showed a DNA ladder, and a more clear DNA ladder was observed in $20 \mu\text{g mL}^{-1}$ HK-NPs-treated cells. No DNA ladder was detected in the samples examined from control cultures (Fig. 4).

SKOV3 ovarian cancer cells were seeded in six-well plates and treated with RPMI-1640, PECE copolymer, F127 and HK-NPs. Using fluorescence microscopy, HK-NPs were shown to induce morphological changes in PI-stained SKOV3 cells characterized

as apoptosis: a brightly red-fluorescent condensed intact or fragmented nuclei, apoptotic bodies and reduction of cell volume. However, these changes were seldom seen in RPMI-1640-treated, PECE-treated or F127-treated cells (Fig. 5).

In addition, a flow cytometry assay of PI staining was used to quantitate the apoptotic cells by observing sub-G1 (apoptotic) cells. As a result, the percentage of sub-G1 cells was 63.7% in HK-NPs-treated SKOV3 cells, *versus* 9.0% in the RPMI-1640-treated group, 15.8% in the PECE-treated group and 16.4% in the F127-treated group (Fig. 6). It was clearly evident that HK-NPs induced a large amount of apoptotic cells. The results obtained from the flow cytometry assay were consistent with morphological changes seen by PI DNA staining and the DNA fragmentation assay. These results were consistent with the fact that HK-NPs induce apoptosis *in vitro*.

3.4 HK-NPs and HK-NPs/hydrogel inhibited OPC *in vivo* and prolonged the survival time of tumor-bearing mice

We have shown that HK-NPs can inhibit SKOV3 cell proliferation and are capable of inducing apoptosis *in vitro*. This led us to evaluate the intraperitoneal chemotherapy effect of HK-NPs and

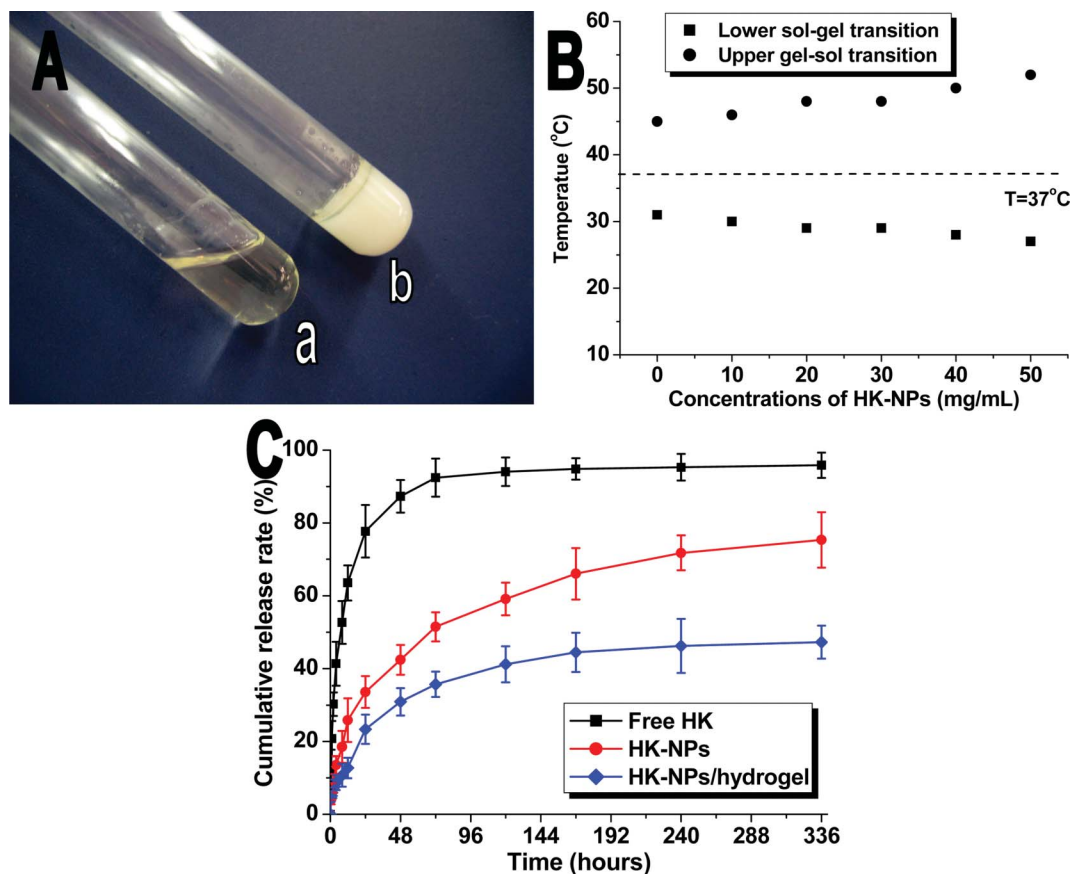


Fig. 2 Characterization of the prepared HK-NPs/hydrogel composite. A: Morphology of HK-NPs/hydrogel (30% wt) at 10 °C (a) or 37 °C (b). B: Effect of HK-NPs content on the sol-gel-sol transition temperature of PCEC hydrogel (30% wt). C: *In vitro* drug release profiles of free HK, HK-NPs, and HK-NPs/hydrogel in PBS solution.

HK-NPs/hydrogel in the mouse model. When the OPC of human ovarian cancer in nude mice was established, intraperitoneal chemotherapy was started 7 days after tumor inoculation. Mice were treated once weekly by injection with 200 μ L NS, 200 μ L blank NPs/hydrogel (30 wt%), 200 μ L free HK (containing HK 10 mg kg^{-1}), 200 μ L HK-NPs iv (containing HK 10 mg kg^{-1}), 200 μ L HK-NPs (containing HK 10 mg kg^{-1}) or 200 μ L HK-NPs/hydrogel (containing HK 10 mg kg^{-1}) for 4 weeks.

In this model, tumor nodules were distributed in the liver, spleen, kidney, intestine, mesentery and pelvic cavity and some of them were fused to masses in the NS and PECE hydrogel groups. A few yellow ascites or bloody ascites were also produced in these two groups. The tumor nodules were significantly less and distribution was limited in the pelvic cavity and mesentery in HK-NPs and HK-NPs/hydrogel groups, and some necrosis was found. No obvious ascites were observed in these two groups. Tumor weight was measured after the mice were sacrificed. The mean tumor weight in HK-NPs/hydrogel-treated mice was 0.22 ± 0.05 g, versus 0.41 ± 0.09 g in HK-NPs-treated mice ($P < 0.05$), 0.72 ± 0.07 g in HK-NPs iv-treated mice ($P < 0.05$), 0.85 ± 0.11 g in free HK-treated mice ($P < 0.05$), 1.49 ± 0.19 g in blank NPs/hydrogel-treated mice ($P < 0.05$) or 1.53 ± 0.10 g in NS-treated mice ($P < 0.05$), (Fig. 7A). There was no significant difference in tumor weight between NS-treated and blank NPs/hydrogel-treated mice ($P > 0.05$). HK-NPs resulted in a decrease in the mean tumor weight compared

with HK-NPs iv, free HK, blank NPs/hydrogel and NS. Furthermore, the HK-NPs/hydrogel group was found to be superior to HK-NPs alone ($P < 0.05$). As shown in Fig. 7C, histological analysis revealed that HK-NPs and HK-NPs/hydrogel-treated tumors had increased cell necrosis.

The beneficial effects of intraperitoneal chemotherapy with HK-NPs and HK-NPs/hydrogel on SKOV3 OPC models were also revealed in the survival time (Fig. 7B). Mice with tumor regression showed longer survival times. Survival of the tumor-bearing mice treated with HK-NPs and HK-NPs/hydrogel was significantly prolonged compared with the control therapies ($P < 0.05$). The HK-NPs/hydrogel group (median survival, 62 days) had better effects on improving survival time than HK-NPs alone (49 days, $P < 0.05$), HK-NPs iv (40 days, $P < 0.05$) or free HK (42 days, $P < 0.05$). There was no significant difference in survival time between NS-treated mice (31 days) and blank NPs/hydrogel-treated mice (33 days, $P > 0.05$, by log-rank test).

3.5 Toxicity observation

No changes in gross measures, such as weight loss, the fur, appetite, status and behavior were indicated in any of the treatment groups (Supplementary Fig. 1†). Furthermore, there was no abnormal finding in H&E histological staining of the heart, lung, liver, spleen, kidney and intestine in each group (Supplementary Fig. 2†).

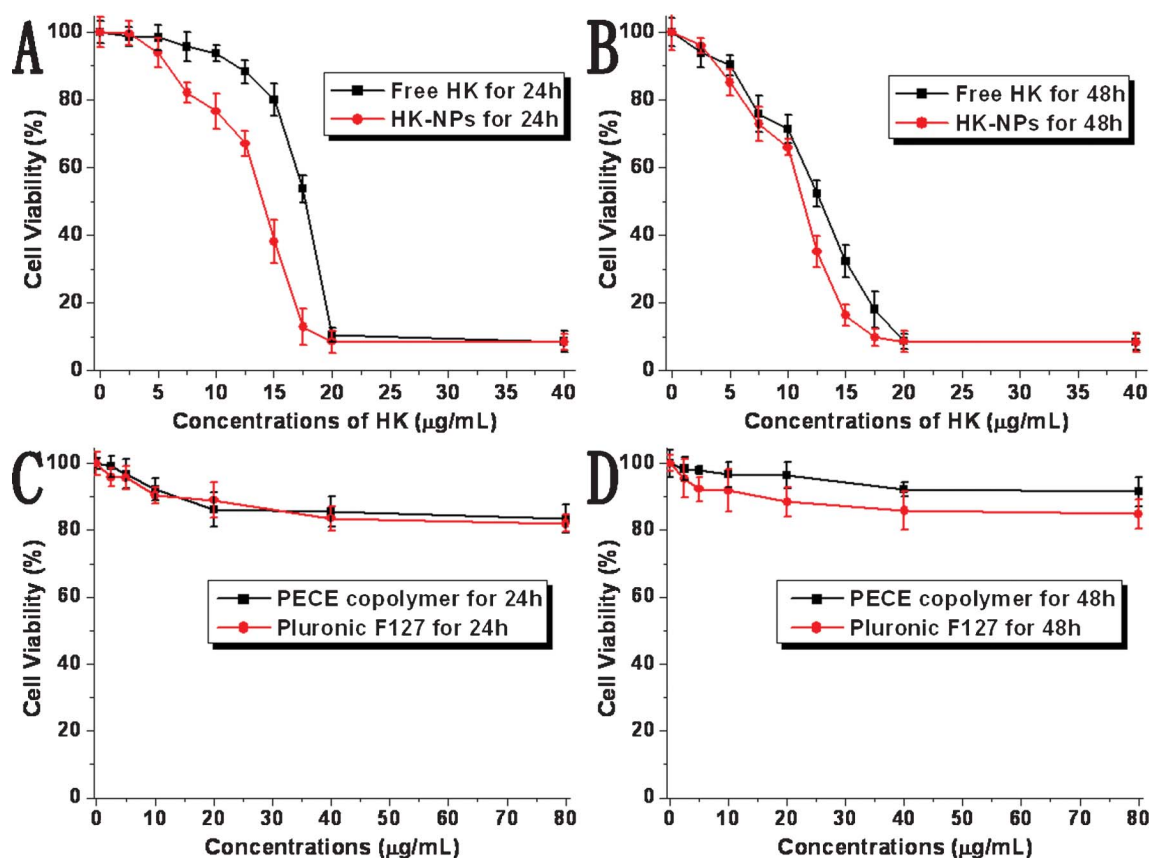


Fig. 3 Inhibitory effect of HK-NPs on the proliferation of SKOV3 cells was assessed by MTT assay. Cells (1×10^4 cells) were incubated with HK-NPs or free HK at the indicated concentrations for 24 h (A) and 48 h (B). Cytotoxicity of F127 and PECE copolymer were also performed for 24 h (C) and 48 h (D). Cell proliferation was expressed as a percentage of viable cells cultured in the absence of drugs. Data are represented as the mean \pm SD ($n = 3$). The results are representative of three separate experiments.

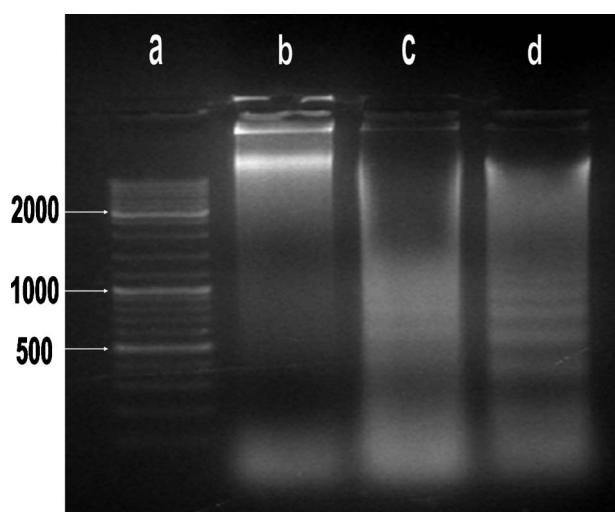


Fig. 4 DNA fragmentation of HK-NPs-treated SKOV3 cells. Lane a: size maker (100 bp DNA ladder). Lane b: SKOV3 cells were treated with RPMI-1640. Lane c: SKOV3 cells were treated with HK-NPs $12.5 \mu\text{g mL}^{-1}$; a DNA ladder on agarose gels is viewed. Lane d: SKOV3 cells were treated with HK-NPs $20 \mu\text{g mL}^{-1}$; a DNA ladder on agarose gels is viewed clearly.

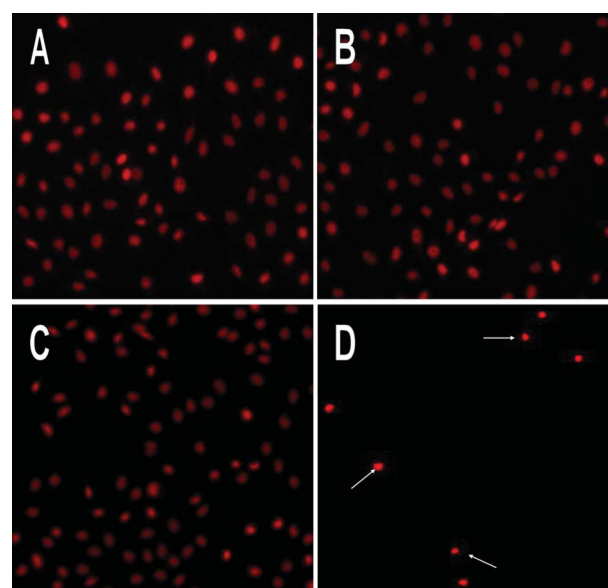


Fig. 5 PI stained fluorescence microscopy of apoptotic nuclei in HK-NPs-treated SKOV3 cells. Cells were treated with RPMI-1640 (A), PECE copolymer (B), F127 (C) and HK-NPs (D) at $12.5 \mu\text{g mL}^{-1}$ for 48 h. HK-NPs induced the morphological changes characterized as apoptosis: a brightly red-fluorescent condensed intact or fragmented nuclei, apoptotic bodies and a reduction of cell volume. Original magnification $\times 200$.

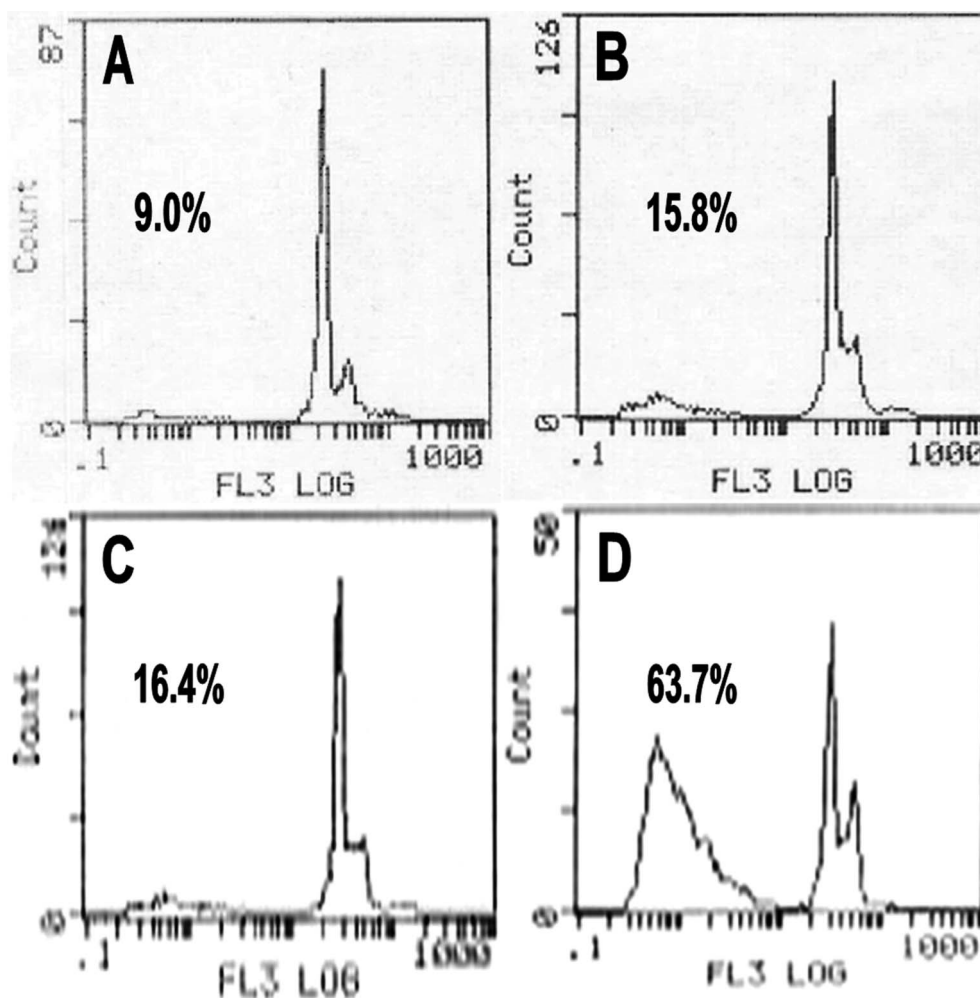


Fig. 6 Flow cytometry assay of PI-stained SKOV3 cells. SKOV3 cells were treated with RPMI-1640 (A), PECE copolymer (B), F127 (C) and HK-NPs (D) at $12.5 \mu\text{g mL}^{-1}$ for 48 h.

3.6 HK-NPs and HK-NPs/hydrogel increased intratumoral apoptosis *in vivo*

To detect the potential mechanisms of the anti-tumor effects of HK-NPs and HK-NPs/hydrogel, we examined their effects on apoptosis, angiogenesis and proliferation.

A TUNEL assay was applied to detect apoptosis of tumor cells in tumor-bearing mice from each group. Viewed with fluorescence microscopy (magnification, $\times 200$), cell nuclei that were stained dark red indicated apoptosis and were recorded as TUNEL-positive nuclei. As shown in Fig. 8, in SKOV3 tumors, the mean apoptotic index \pm SD of cancer cells treated with NS was $4.80 \pm 1.30\%$ versus $5.20 \pm 2.39\%$ in the blank NPs/hydrogel-treated group, $18.60 \pm 4.20\%$ in the free HK-treated group, $16.90 \pm 3.80\%$ in the HK-NPs iv-treated group, $31.40 \pm 7.13\%$ in the HK-NPs-treated group and $54.40 \pm 6.88\%$ in the HK-NPs/hydrogel-treated group. Significant increases of TUNEL-positive nuclei were found in the HK-NPs-treated group and HK-NPs/hydrogel-treated group compared with the NS-treated, blank NPs/hydrogel-treated, free HK-treated and HK-NPs iv-treated groups ($P < 0.05$). Moreover, the use of HK-NPs/hydrogel as a controlled drug delivery system had a better apoptotic induction effect than HK-NPs alone ($P < 0.05$). There

was no significant difference between the NS-treated and blank NPs/hydrogel-treated groups ($P > 0.05$).

3.7 HK-NPs and HK-NPs/hydrogel inhibited intratumoral angiogenesis

Angiogenesis in tumor tissues was evaluated by quantifying MVD. In paraffin embedded sections a single microvessel was defined as a discrete cluster or a single cell staining positive for CD34, and the presence of a lumen was required for scoring the structure as a microvessel. 10 random 0.159 mm^2 fields at $\times 100$ magnification were examined for each tumor. As shown in Fig. 9, in SKOV3 tumors, MVD \pm SD of cancer cells treated with NS was 61.20 ± 5.12 versus 60.80 ± 11.92 in the blank NPs/hydrogel-treated group, 40.60 ± 3.90 in the free HK-treated group, 44.30 ± 5.60 in the HK-NPs iv-treated group, 31.20 ± 5.50 in the HK-NPs-treated group and 18.60 ± 5.94 in the HK-NPs/hydrogel-treated group. Significant inhibition of angiogenesis in SKOV3 tumors was found in the HK-NPs-treated and HK-NPs/hydrogel-treated groups compared with the HK-NPs iv-treated, free HK-treated, blank NPs/hydrogel-treated and NS-treated groups ($P < 0.05$). Moreover, HK-NPs/hydrogel as a controlled drug delivery system appeared to

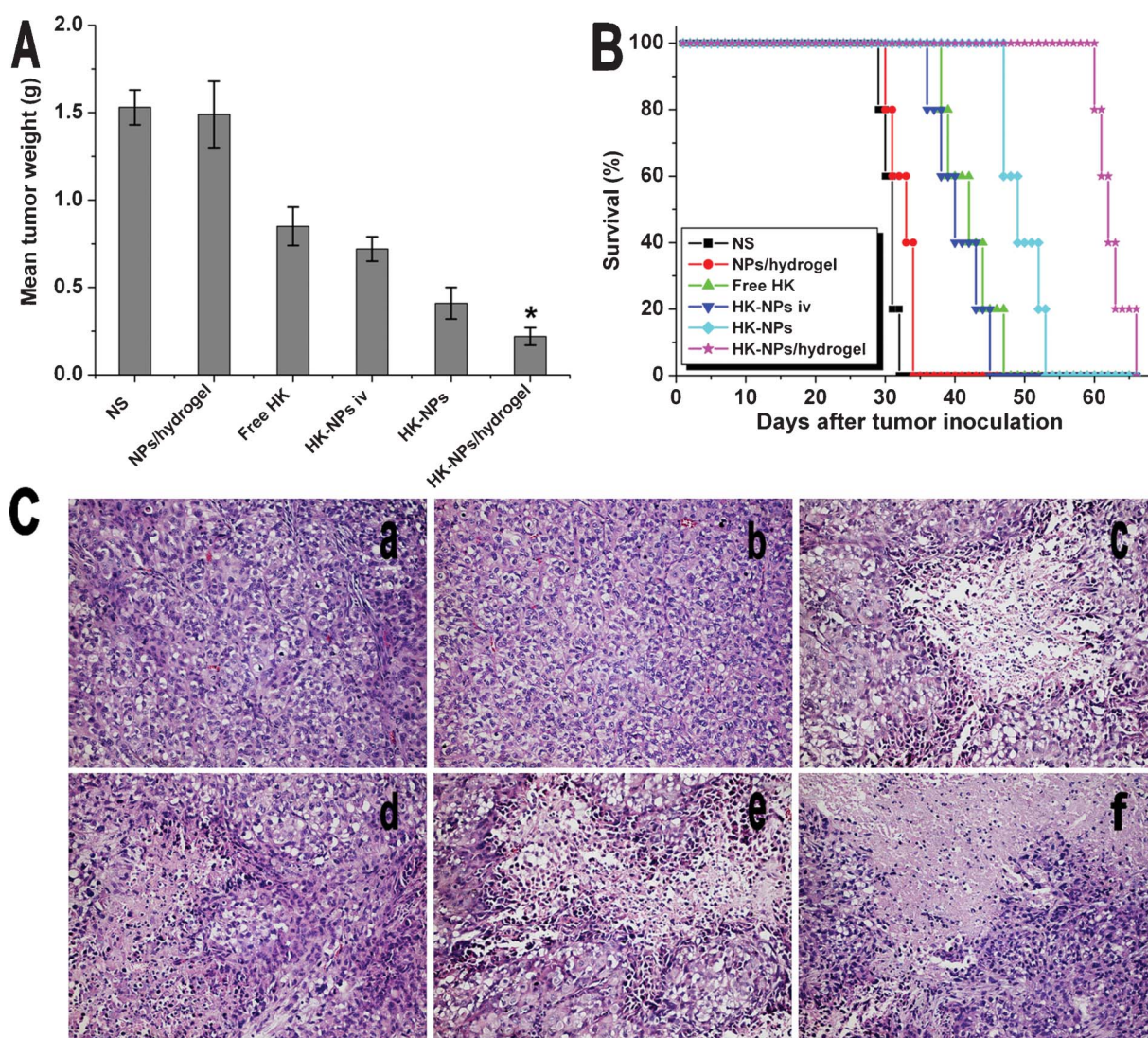


Fig. 7 Therapeutic efficacy of HK-NPs and HK-NPs/hydrogel in the OPC mice model. A: Mean tumor weight in each group. B: Survival curve of each group. C: Sections of tumors stained by H&E in NS (a), blank NPs/hydrogel (b), free HK (c), HK-NPs iv (d), HK-NPs (e) and HK-NPs/hydrogel (f) treated groups.

have a better angiogenesis inhibition effect than HK-NPs alone ($P < 0.05$). There was no significant difference between the NS-treated and blank NPs/hydrogel-treated groups ($P > 0.05$).

3.8 HK-NPs and HK-NPs/hydrogel inhibited cell proliferation

Using immunochemistry with proliferating cell nuclear antigen (PCNA), we detected cell proliferation activity. The microscopic examination of PCNA staining of tumors showed weak PCNA immunoreactivity in HK-NPs-treated and HK-NPs/hydrogel-treated groups when compared with the control groups (Fig. 10). In SKOV3 tumors, PCNA LI \pm SD of cancer cells treated with NS was $75.0 \pm 8.94\%$ versus $69.60 \pm 5.98\%$ in the blank NPs/hydrogel-treated group, $42.20 \pm 5.31\%$ in the free HK-treated group, $47.40 \pm 6.36\%$ in the HK-NPs iv-treated group, $29.40 \pm 5.18\%$ in the HK-NPs-treated group and $14.00 \pm 6.40\%$ in the HK-NPs/hydrogel-treated group. In SKOV3 tumors, the HK-NPs-treated group and the HK-NPs/hydrogel-treated group showed a decrease in cell proliferation compared with other

groups ($P < 0.05$). The HK-NPs/hydrogel showed a more pronounced anti-cell proliferation effect than HK-NPs alone ($P < 0.05$). There was no significant difference between the NS-treated and blank NPs/hydrogel-treated groups ($P > 0.05$).

4 Discussion

Ovarian cancer is the leading cause of death from a gynecological cancer.¹ Despite significant advances in modern surgical interventions and contemporary chemotherapy, the prognosis remains poor. The 5-year overall survival rate of patients with the advanced disease (stage III and IV) is only 15% to 25%. The lack of effective screening methods means that approximately 70% of patients present with the advanced stages of the disease. The high incidence of chemotherapy resistance and low-volume residual disease in initial surgery also reflects the high relapse rate and mortality rate.³ Ovarian cancer commonly spreads within the peritoneal cavity. Most recent studies show that IP treatment resulted in a significant increase in both progression-free and

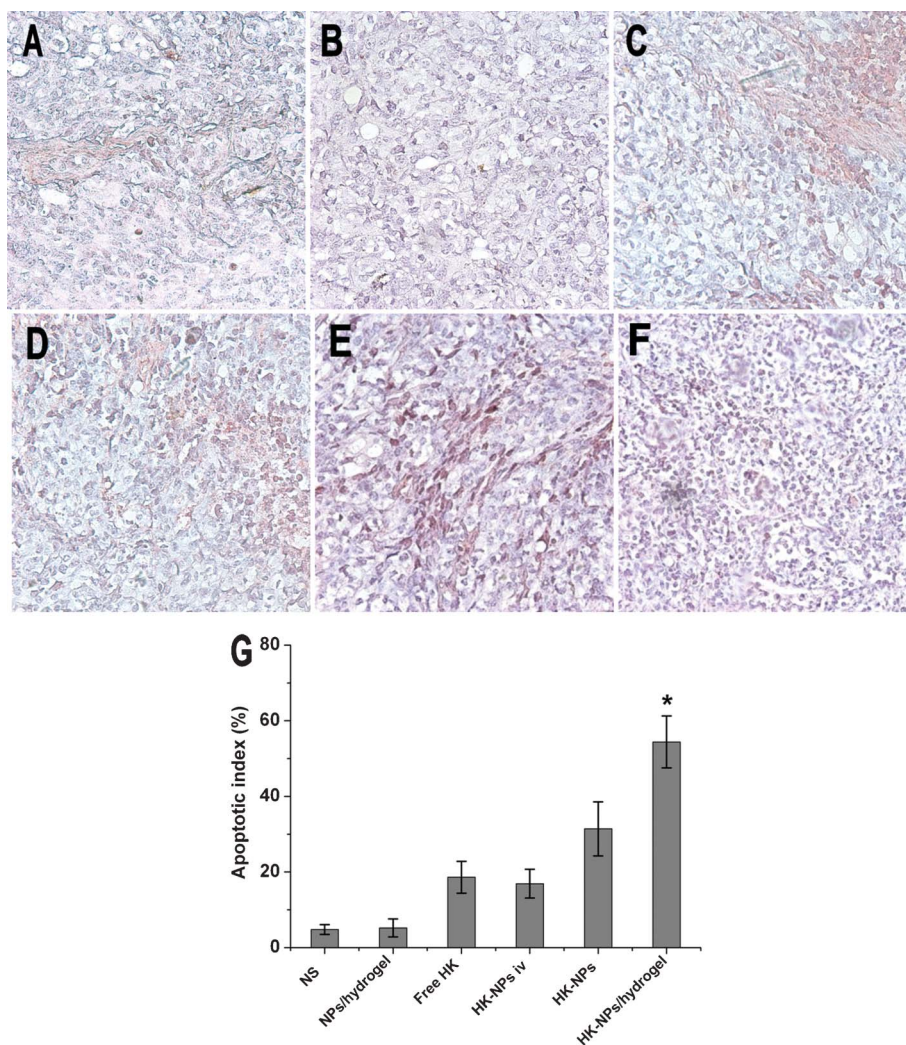


Fig. 8 TUNEL staining of tumor tissues from each group. Representative sections were taken from tumor tissue of NS (A), blank NPs/hydrogel (B), free HK (C), HK-NPs iv (D), HK-NPs (E), and HK-NPs/hydrogel (F) treated groups, respectively. The percentage of apoptotic cells in HK-NPs treatment groups markedly increased compared with controls ($P < 0.05$), with an even greater induction of apoptosis in the HK-NPs/hydrogel-treated group (G).

overall survival of the patients.³⁶ Although modern surgical approaches could be supplemented by administration of chemotherapy to the low-volume residual disease in the peritoneal cavity, increased toxicity caused by the high-dose intraperitoneal drug administration and catheter-related complications have been reported, including neutropenia, neuropathy, infection, abdominal pain, bowel perforation and bowel obstruction.^{2,37} Many patients have had to give up the assigned cycles of IP therapy because of the adverse reactions.⁶

The present study explored the feasibility of using the novel controlled-release drug-delivery system, HK-NPs/hydrogel, for IP chemotherapy and the therapeutic effects of experimentally-induced human ovarian cancer. HK is a multifunctional drug and it was demonstrated to show great potential anti-tumor activity. It has been reported to exhibit a potent cytotoxic activity by inducing cell apoptosis in RKO, SW480, LS180, CH27, H460 and H1299 cell lines in a dose- and time-dependent manner. HK-mediated cytotoxicity occurred at a concentration of $5 \mu\text{g mL}^{-1}$ and above.^{38,39} Previous studies in our laboratory

suggest a significant inhibitory effect of HK on the proliferation of human ovarian cancer SKOV3 cells. The IC₅₀ at 24 h was determined to be $14\text{--}20 \mu\text{g mL}^{-1}$.⁴⁰ However, the high hydrophobicity of HK limited its further clinical application. To overcome this problem, HK-NPs were prepared. The obtained HK-NPs could be well-dispersed in water and are stable. The maximum possible concentration was up to 25 mg mL^{-1} . The average particle size was about 33.36 nm and the nanoparticles had a small negative zeta potential (about -0.270 mV) close to neutral.²⁶ In our study, HK-NPs showed no significant difference in the cytotoxic activity compared with free HK on SKOV3 cells. Furthermore, the cytotoxic effect was enhanced by providing slow-release of an encapsulated drug, resulting in sustained exposure to tumor cells.⁴¹

In situ gel-forming sustained drug delivery systems have received considerable attention over past decades.⁴² The thermosensitive hydrogel has been extensively studied for its potential biomedical applications. The PECE hydrogel prepared in this study was composed of PEG and PCL, which are widely

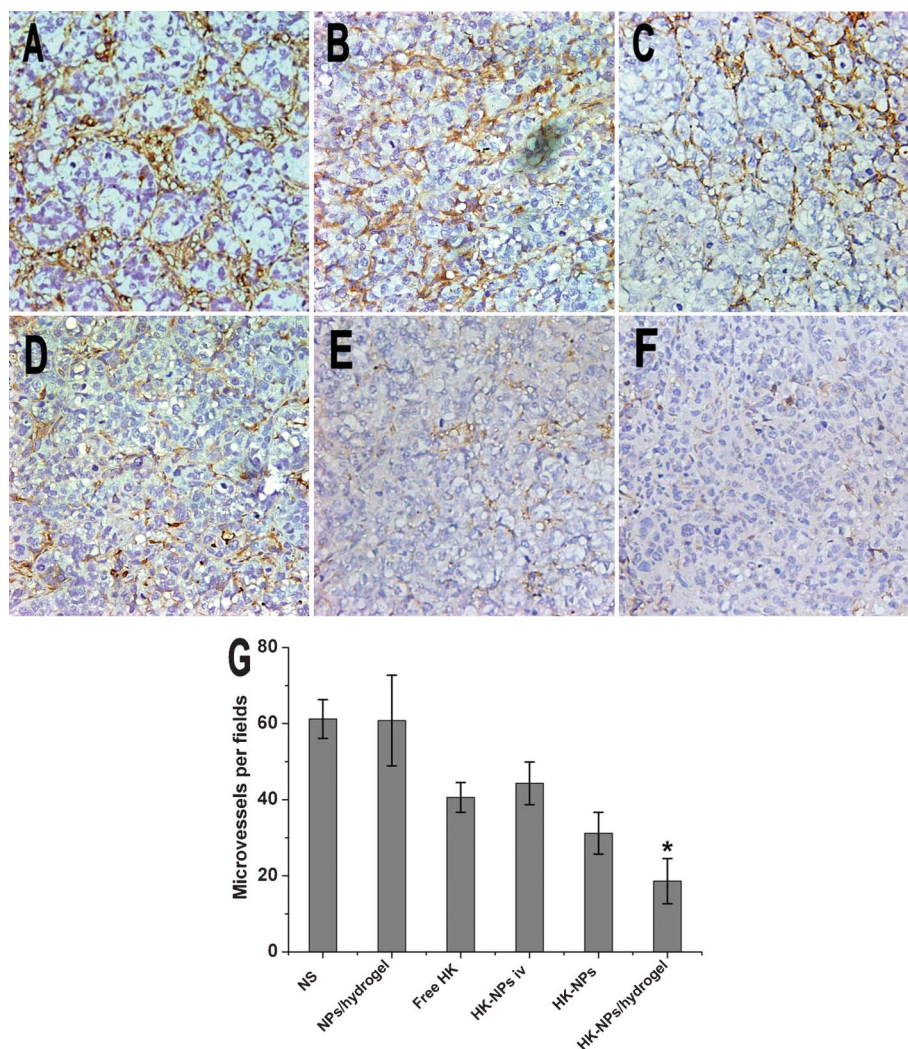


Fig. 9 Inhibition of intratumoral angiogenesis assayed by CD34 staining of microvessels. Representative sections were taken from SKOV3 tumor tissue of NS (A), blank NPs/hydrogel (B), free HK (C), HK-NPs iv (D), HK-NPs (E), and HK-NPs/hydrogel (F) treated groups. The number of microvessels was significantly smaller in the HK-NPs-treated group compared with controls ($P < 0.05$), and in the HK-NPs/hydrogel-treated group a better anti-angiogenesis effect was observed (G).

used in FDA-approved drug preparations. Based on previous studies, the MTD of PECE hydrogel is higher than 10 g kg^{-1} body weight, which is much higher than the dose used as a drug carrier. PECE hydrogel seems a safe candidate for use as a sustained drug delivery system. The special thermosensitive sol-gel transition temperature of biodegradable PECE hydrogel was nearly at 37°C . It is a free-flowing sol at room temperature and becomes gel at body temperature. Therefore, it can easily mix with drugs and can be injected by syringe *in vitro*, while forming a deposition at the target location *in vivo*.⁴³ HK-NPs/hydrogel could release HK in an extended period at effective levels *in vivo*, thus avoiding its release in bursts when HK is delivered directly.

In our previous work, liposomal HK was prepared and used for treatment of various tumors, such as lung cancer, colon cancer and breast cancer. In this work, polymeric HK-NPs were prepared and used for treatment of ovarian cancer, and *in vitro* release behavior and therapeutic efficiency of HK-NPs, HK-NPs/hydrogel, liposomal HK and liposomal HK/hydrogel were investigated. *In vitro* release profiles showed that the release rate

of liposomal HK was faster than that of HK-NPs, but no significant differences were observed between liposomal HK/hydrogel and HK-NPs/hydrogel (Supplementary Fig. 3†). For *in vivo* tests, tumor weight in the HK-NPs group is significant lower than that in the liposomal HK group, but there is no significant differences between liposomal HK/hydrogel and HK-NPs/hydrogel (Supplementary Fig. 4†).

The present studies demonstrate that intraperitoneal therapy with HK-NPs resulted in inhibition of SKOV3 ovarian cancer growth *in vivo* and significantly prolonged the survival time of tumor-bearing mice, compared with the NS-treated and blank NPs/hydrogel-treated controls. Besides, HK-NPs/hydrogel as a sustained drug delivery system *via* intrapleural administration was more efficient therapeutically and significantly improved the survival rate. The *in vivo* anti-tumor mechanism of HK-NPs and HK-NPs/hydrogel for ovarian cancer remains not completely clear. A TUNEL assay was used to determine whether HK-NPs and HK-NPs/hydrogel increased intratumoral apoptosis *in vivo*. The result was consistent with the *in vitro* findings described

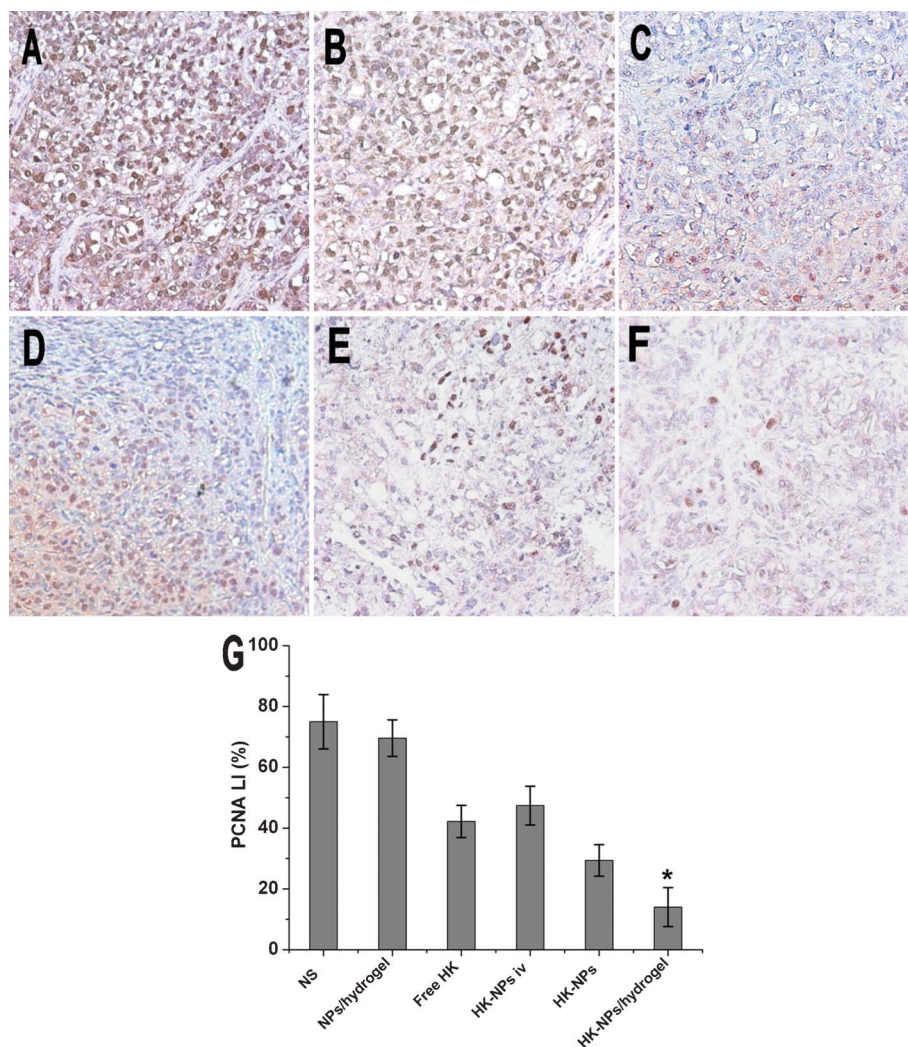


Fig. 10 Inhibition of cell proliferation assayed by PCNA staining. Representative sections were taken from SKOV3 tumor tissue of NS (A), blank NPs/hydrogel (B), free HK (C), HK-NPs iv (D), HK-NPs (E) and HK-NPs/hydrogel (F) treated groups. The PCNA-positive cells in HK-NPs and HK-NPs/hydrogel groups were significantly less when compared with controls ($P < 0.05$), and the HK-NPs/hydrogel-treated group showed a better anti-cell proliferation effect (G).

above and the apoptosis-inducing ability of HK reported previously.^{44,45}

Angiogenesis plays an important role in tumor growth and metastasis. The anti-angiogenic activity of HK-NPs and HK-NPs/hydrogel were evaluated by quantifying MVD. We found that HK-NPs and HK-NPs/hydrogel were efficient at blocking the formation of new blood vessels in tumors. Moreover, HK-NPs and HK-NPs/hydrogel could inhibit tumor cell proliferation and limit the emergence of malignant cell populations, as confirmed by PCNA staining, which was consistent with the *in vitro* findings described above. In addition, more apparent anti-tumor activities were found in the HK-NPs/hydrogel-treated group than the HK-NPs-treated group *in vivo*. The sustained delivery of HK may contribute to the better anti-tumor effect.

5 Conclusions

Even in light of the limitations (such as the incomplete understanding of the anti-tumor mechanism of HK and the

relation between anti-tumor effect and sustained delivery of HK), we can provide some important conclusions. Anti-tumor and anti-angiogenesis effects of HK-NPs and HK-NPs/hydrogel for treatment of human ovarian cancer by intraperitoneal administration were investigated. Our results showed HK-NPs/hydrogel, as a sustained drug delivery system, could enhance the therapeutic effects and diminish the side effects of HK. This drug delivery system with various potential anti-tumor abilities is novel and is potentially an attractive intraperitoneal therapeutic candidate for ovarian tumor treatment in clinical practice.

Declaration of interest statement

The authors report no conflicts of interest. The authors alone are responsible for the content and writing of the paper.

References

- 1 R. Siegel, D. Naishadham and A. Jemal, *Ca-Cancer J. Clin.*, 2012, **62**, 10–29.

- 2 S. M. Kehoe, N. L. Williams, R. Yakubu, D. A. Levine, D. S. Chi, P. J. Sabbatini, C. A. Aghajanian, R. R. Barakat and N. R. Abu-Rustum, *Gynecol. Oncol.*, 2009, **113**, 228–232.
- 3 P. J. Frederick, J. M. Straughn Jr., R. D. Alvarez and D. J. Buchsbaum, *Gynecol. Oncol.*, 2009, **113**, 384–390.
- 4 D. S. Alberts, P. Y. Liu, E. V. Hannigan, R. O'Toole, S. D. Williams, J. A. Young, E. W. Franklin, D. L. Clarke-Pearson, V. K. Malviya and B. DuBeshter, *N. Engl. J. Med.*, 1996, **335**, 1950–1955.
- 5 M. Markman, B. N. Bundy, D. S. Alberts, J. M. Fowler, D. L. Clark-Pearson, L. F. Carson, S. Wadler and J. Sickel, *J. Clin. Oncol.*, 2001, **19**, 1001–1007.
- 6 D. K. Armstrong, B. Bundy, L. Wenzel, H. Q. Huang, R. Baergen, S. Lele, L. J. Copeland, J. L. Walker and R. A. Burger, *N. Engl. J. Med.*, 2006, **354**, 34–43.
- 7 K. Jaaback, N. Johnson and T. A. Lawrie, *Cochrane Database Syst Rev*, 2011, **11**, CD005340.
- 8 M. Markman and J. L. Walker, *J. Clin. Oncol.*, 2006, **24**, 988–994.
- 9 L. M. Landrum, M. A. Gold, K. N. Moore, T. K. Myers, D. S. McMeekin and J. L. Walker, *Gynecol. Oncol.*, 2008, **108**, 342–347.
- 10 L. M. Landrum, J. Hyde Jr., R. S. Mannel, D. S. McMeekin, K. N. Moore and J. L. Walker, *Gynecol. Oncol.*, 2011, **122**, 527–531.
- 11 S. Ponnuram, J. M. Mammen, S. Ramalingam, Z. He, Y. Zhang, S. Umar, D. Subramaniam and S. Anant, *Mol. Cancer Ther.*, 2012.
- 12 J. W. Lin, J. T. Chen, C. Y. Hong, Y. L. Lin, K. T. Wang, C. J. Yao, G. M. Lai and R. M. Chen, *Neuro-Oncology*, 2012, **14**, 302–314.
- 13 P. Steinmann, D. K. Walters, E. A. MJ, I. J. Banke, U. Ziegler, B. Langsam, J. Arbiser, R. Muff, W. Born and B. Fuchs, *Cancer*, 2011.
- 14 T. Singh and S. K. Katiyar, *Int. J. Oncol.*, 2011, **38**, 769–776.
- 15 P. W. Mannal, J. Schneider, A. Tangada, D. McDonald and D. W. McFadden, *Journal of Surgical Oncology*, 2011, **104**, 260–264.
- 16 S. Arora, A. Bhardwaj, S. K. Srivastava, S. Singh, S. McClellan, B. Wang and A. P. Singh, *PLoS One*, 2011, **6**, e21573.
- 17 L. L. Han, L. P. Xie, L. H. Li, X. W. Zhang, R. Q. Zhang and H. Z. Wang, *Environ. Toxicol. Pharmacol.*, 2009, **28**, 97–103.
- 18 Y. Wang, Z. Yang and X. Zhao, *Toxicol. Mech. Methods*, 2010, **20**, 234–241.
- 19 Q. Q. Jiang, L. Y. Fan, G. L. Yang, W. H. Guo, W. L. Hou, L. J. Chen and Y. Q. Wei, *BMC Cancer*, 2008, **8**, 242.
- 20 H. Luo, Q. Zhong, L. J. Chen, X. R. Qi, A. F. Fu, H. S. Yang, F. Yang, H. G. Lin, Y. Q. Wei and X. Zhao, *J. Cancer Res. Clin. Oncol.*, 2008, **134**, 937–945.
- 21 Y. Liu, L. Chen, X. He, L. Fan, G. Yang, X. Chen, X. Lin, L. Du, Z. Li, H. Ye, Y. Mao, X. Zhao and Y. Wei, *Int. J. Gynecol. Cancer*, 2008, **18**, 652–659.
- 22 C. Gong, X. Wei, X. Wang, Y. Wang, G. Guo, Y. Mao, F. Luo and Z. Qian, *Nanotechnology*, 2010, **21**, 215103.
- 23 C. Y. Gong, S. Shi, P. W. Dong, B. Kan, M. L. Gou, X. H. Wang, X. Y. Li, F. Luo, X. Zhao, Y. Q. Wei and Z. Y. Qian, *Int. J. Pharm.*, 2009, **365**, 89–99.
- 24 C. Y. Gong, Y. J. Wang, X. H. Wang, X. W. Wei, Q. J. Wu, B. L. Wang, P. W. Dong, L. J. Chen, F. Luo and Z. Y. Qian, *J. Nanopart. Res.*, 2011, **13**, 721–731.
- 25 A. K. Sood, E. A. Seftor, M. S. Fletcher, L. M. Gardner, P. M. Heidger, R. E. Buller, R. E. Seftor and M. J. Hendrix, *Am. J. Pathol.*, 2001, **158**, 1279–1288.
- 26 M. L. Gou, M. Dai, X. Y. Li, X. H. Wang, C. Y. Gong, Y. Xie, K. Wang, X. Zhao, Z. Y. Qian and Y. Q. Wei, *J. Mater. Sci.: Mater. Med.*, 2008, **19**, 2605–2608.
- 27 C. Gong, S. Shi, X. Wang, Y. Wang, S. Fu, P. Dong, L. Chen, X. Zhao, Y. Wei and Z. Qian, *J. Phys. Chem. B*, 2009, **113**, 10183–10188.
- 28 Y. Q. Wei, Q. R. Wang, X. Zhao, L. Yang, L. Tian, Y. Lu, B. Kang, C. J. Lu, M. J. Huang, Y. Y. Lou, F. Xiao, Q. M. He, J. M. Shu, X. J. Xie, Y. Q. Mao, S. Lei, F. Luo, L. Q. Zhou, C. E. Liu, H. Zhou, Y. Jiang, F. Peng, L. P. Yuan, Q. Li, Y. Wu and J. Y. Liu, *Nat. Med.*, 2000, **6**, 1160–1166.
- 29 Y. Q. Wei, M. J. Huang, L. Yang, X. Zhao, L. Tian, Y. Lu, J. M. Shu, C. J. Lu, T. Niu, B. Kang, Y. Q. Mao, F. Liu, Y. J. Wen, S. Lei, F. Luo, L. Q. Zhou, F. Peng, Y. Jiang, J. Y. Liu, H. Zhou, Q. R. Wang, Q. M. He, F. Xiao, Y. Y. Lou, X. J. Xie, Q. Li, Y. Wu, Z. Y. Ding, B. Hu, M. Hu and W. Zhang, *Proc. Natl. Acad. Sci. U. S. A.*, 2001, **98**, 11545–11550.
- 30 Y. Q. Wei, X. Zhao, Y. Kariya, H. Fukata, K. Teshigawara and A. Uchida, *Cancer Res.*, 1994, **54**, 4952–4957.
- 31 W. Gorczyca, J. Gong, B. Ardel, F. Traganos and Z. Darzynkiewicz, *Cancer Res.*, 1993, **53**, 3186–3192.
- 32 X. J. Lin, X. C. Chen, L. Wang, Y. Q. Wei, B. Kan, Y. J. Wen, X. He and X. Zhao, *J. Exp. Clin. Cancer Res.*, 2007, **26**, 467–474.
- 33 J. Halder, A. A. Kamat, C. N. Landen Jr., L. Y. Han, S. K. Lutgendorf, Y. G. Lin, W. M. Merritt, N. B. Jennings, A. Chavez-Reyes, R. L. Coleman, D. M. Gershenson, R. Schmandt, S. W. Cole, G. Lopez-Berestein and A. K. Sood, *Clin. Cancer Res.*, 2006, **12**, 4916–4924.
- 34 C. Y. Gong, P. W. Dong, S. Shi, S. Z. Fu, J. L. Yang, G. Guo, X. Zhao, Y. Q. Wei and Z. Y. Qian, *J. Pharm. Sci.*, 2009, **98**, 3707–3717.
- 35 C. Y. Gong, S. Shi, X. H. Wang, Y. J. Wang, S. Z. Fu, P. W. Dong, L. J. Chen, X. Zhao, Y. Q. Wei and Z. Y. Qian, *J. Phys. Chem. B*, 2009, **113**, 10183–10188.
- 36 R. J. Morgan Jr., R. D. Alvarez, D. K. Armstrong, B. Boston, R. A. Burger, L. M. Chen, L. Copeland, M. A. Crispens, D. Gershenson, H. J. Gray, P. W. Grigsby, A. Hakam, L. J. Havrilesky, C. Johnston, S. Lele, U. A. Matulonis, D. M. O'Malley, R. T. Penson, S. W. Remmenga, P. Sabbatini, R. J. Schilder, J. C. Schink, N. Teng and T. L. Werner, *J. Natl. Compr. Canc. Netw.*, 2011, **9**, 82–113.
- 37 L. Elit, T. K. Oliver, A. Covens, J. Kwon, M. F. Fung, H. W. Hirte and A. M. Oza, *Cancer*, 2007, **109**, 692–702.
- 38 T. Wang, F. Chen, Z. Chen, Y. F. Wu, X. L. Xu, S. Zheng and X. Hu, *World J. Gastroenterol.*, 2004, **10**, 2205–2208.
- 39 S. E. Yang, M. T. Hsieh, T. H. Tsai and S. L. Hsu, *Biochem. Pharmacol.*, 2002, **63**, 1641–1651.
- 40 Z. Li, Y. Liu, X. Zhao, X. Pan, R. Yin, C. Huang, L. Chen and Y. Wei, *Eur. J. Obstet. Gynecol. Reprod. Biol.*, 2008, **140**, 95–102.
- 41 N. Tang, G. Du, N. Wang, C. Liu, H. Hang and W. Liang, *J. Natl. Cancer Inst.*, 2007, **99**, 1004–1015.
- 42 C. B. Liu, C. Y. Gong, M. J. Huang, J. W. Wang, Y. F. Pan, Y. D. Zhang, G. Z. Li, M. L. Gou, K. Wang, M. J. Tu, Y. Q. Wei and Z. Y. Qian, *J. Biomed. Mater. Res. B Appl. Biomater.*, 2008, **84**, 165–175.
- 43 C. Gong, S. Shi, P. Dong, B. Kan, M. Gou, X. Wang, X. Li, F. Luo, X. Zhao, Y. Wei and Z. Qian, *Int. J. Pharm.*, 2009, **365**, 89–99.
- 44 T. E. Battle, J. Arbiser and D. A. Frank, *Blood*, 2005, **106**, 690–697.
- 45 K. Ishitsuka, T. Hideshima, M. Hamasaki, N. Raje, S. Kumar, H. Hideshima, N. Shiraishi, H. Yasui, A. M. Roccaro and P. Richardson, *Blood*, 2005, **106**, 1794–1800.